Journal of Marine Research, 51, 797–818, 1993

Advection and eddy mixing in the Mediterranean salt tongue

by Michael A. Spall[1], Philip L. Richardson[1] and James Price[1]

ABSTRACT

Lagrangian trajectories from the SOFAR float Mediterranean outflow experiment are used to estimate the low frequency variability and mixing in the vicinity of the Mediterranean salt tongue. Two dominant patterns of Lagrangian variability are observed, (1) nearly zonal low frequency motions and (2) wave-like oscillations with northwest to southeast orientation. The zonal motions are found near the core of the salt tongue in the Canary Basin while the oscillations are generally found to the south and east. It is suggested that the zonal motions are the result of baroclinic instability of the large-scale flow. They have zonally enhanced low frequency variability (periods greater than 200 days) and nearly isotropic mesoscale variability (periods 50 to 200 days). The wave motions are believed to be the signature of radiating baroclinic Rossby waves generated to the south at the Cape Verde Frontal Zone. They are strongly peaked at the mesoscale band and have an essentially isotropic low frequency component. Integral time scales for the zonal motions are relatively long (23 and 13 days for the zonal and meridional directions) while for the wave motions they are short (7.7 and 5.0 days). The resulting eddy diffusivities are found to be non-isotropic and non-homogeneous with $(K_{xx}, K_{yy}) = (21 \text{ and } 8.4 \times 10^6 \text{ cm}^2 \text{ s}^{-1})$ in the core of the salt tongue (mainly zonal motions) and $(K_{xx}, K_{yy}) = (4.3 \text{ and } 3.5 \times 10^6 \text{ cm}^2 \text{ s}^{-1})$ to the south of the core (mainly wave-like motions). A simple scale analysis indicates that these time dependent motions play the dominant role in the spread of the Mediterranean salt tongue in both the zonal and meridional directions.

1. Introduction

Advection and mixing processes in the ocean are of fundamental importance as they influence dynamically active tracers such as temperature, salinity, and potential vorticity, as well as passive tracers such as oxygen and nutrients. The Mediterranean salt tongue is an attractive region to study the relative influences of advection and diffusion for several reasons. The Mediterranean outflow is a major source of high salinity water to the worlds oceans and the resulting salt tongue is a dominant signal of the North Atlantic hydrography. In addition, there is a relatively large amount of data available in this region. Because it is removed from near surface forcing and western boundary currents, this area is well suited to the application of classical

1. Woods Hole Oceanographic Institution, Woods Hole, Massachusetts, 02543, U.S.A.

mixing theories. Although eddy kinetic energy levels within the subtropical gyre are much less than that in the vicinity of western boundary currents (Schmitz *et al.,* 1988), the eddy kinetic energy is generally an order of magnitude greater than the mean. This suggests that, although the eddies are relatively weak, the mixing due to time dependent motions is important in determining the steady balance of tracers and momentum. Much of our present understanding of how time dependent motions might lead to the transport of passive tracers stems from the original work of Taylor (1921). In relating particle transport to the basic statistical quantities of the variability, Taylor assumed that the time dependent motion was represented by homogeneous, stationary turbulence. While this is not strictly met in many regions of the worlds oceans, particularily near western boundary currents, there have been several attempts to apply these theories to estimate the mixing properties within subtropical gyres based on both observations (Freeland *et al.,* 1975; Rossby *et al.,* 1983; Riser and Rossby, 1983; Krauss and Böning, 1987) and models (Haidvogel and Keffer, 1984; Böning and Cox, 1988). The present study adds to these previous works and is the first attempt to directly estimate the relative contributions of the mean and time dependent motions to the dispersion of particles in the Mediterranean salt tongue.

The basic idea that advective and diffusive components of the flow spread salt from the near coastal region off Portugal into the interior of the North Atlantic has been used by many investigators to study the dynamics of the Mediterranean salt tongue. Defant (1955) first used an assumed advective/diffusive balance to model the salt tongue. Needler and Heath (1975) used a uniform westward mean flow and the observed climatological salinity distribution to obtain estimates of horizontal and vertical eddy diffusivities. Richardson and Mooney (1975) studied the qualitative effects of diffusion on the steady state distribution of tongue-like features extending into the interior from the eastern boundary. Hogg (1987) used a least-squares inversion of the steady advection-diffusion equation to derive a horizontal velocity field and diffusivities consistent with isotropic Laplacian diffusion and the climatological salinity distribution. Armi and Haidvogel (1982) demonstrated that variable and anisotropic diffusion coefficients could generate tongue-like features on the same order of magnitude as the estimated mean circulation. These studies have demonstrated that steady advection with Laplacian diffusion can produce results which are qualitatively consistent with observations but that the influences of non-homogeneity and anisotropy may be as important as the mean circulation.

Direct estimates of the relative contributions of mean and eddy components of the flow to particle dispersion in the salt tongue have not been available. Krauss and Böning (1987) studied the Lagrangian properties of the near surface flow in the North Atlantic between Newfoundland and the Canary Basin, extending into the region over the salt tongue. They found a nearly linear relationship between the diffusion coefficient and the eddy kinetic energy over the entire range of their data, implying uniform integral time scales. There was also clear evidence of anisotropy

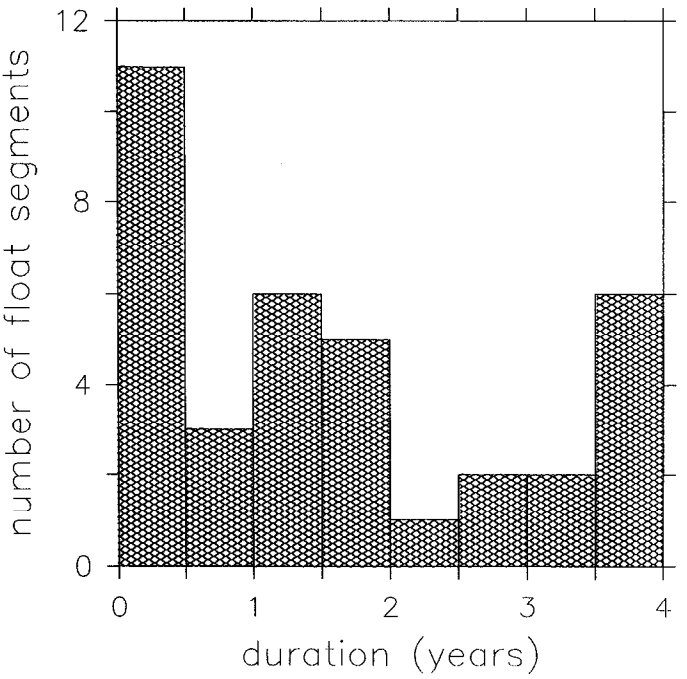

Figure 1. Histogram of the duration of float segments for all floats not in Meddies.

with zonal mixing larger than the meridional mixing. Böning and Cox (1988) simulated the Lagrangian dispersion of parcels in an eddy resolving general circulation model and found that, in the eastern basin, the mixing due to the eddy field was anisotropic, surface intensified, and varied with latitude. Peclet numbers on the order of 2–3 were estimated for the flow, indicating that both mean and eddy components are important.

The Mediterranean outflow experiment was carried out between 1984 and 1988 to observe the long-term motion of SOFAR floats released within the Mediterranean salt tongue. The primary goal of the experiment was to understand how advection and diffusion produce the westward extension of the salt tongue. Altogether, 32 floats were launched near 1100 m, including a cluster of 14 floats near 32N, 24W with nearest neighbors at 20 km spacing, 10 additional floats along an approximately meridional line near 24W with 200 km meridional spacing, and 8 floats in Meddies (submesoscale lenses of Mediterranean water). The experiment was quite successful from a technical point of view, returning approximately 60 float years of data. A histogram of duration of float track segments is shown in Figure 1. Several float tracks have been been broken up into segments in instances when there was a loss of data for several days. Each of the resulting segments is treated as a separate float track in this paper. Six floats lasted the duration of the experiment, between 3.5 and 4 years, while over half returned time series of over 1 year. Many of the short segments

(less than 0.5 years) are actually part of a longer time series but are isolated here due to data loss. The present analysis will concentrate only on those floats which were not in Meddies, or which were initially placed in Meddies but sometime during the experiment came out of them. A discussion of those floats in Meddies is given by Richardson *et al.* (1989) and Armi *et al.* (1989). Preliminary results from the SOFAR float experiment and current meter data are discussed by Schmitz *et al.* (1988). Details of the experiment and data processing are described by Zemanovic *et al.* (1990).

A summary of the Lagrangian float tracks is given in Section 2 and the spatial and temporal distributions of the eddy kinetic energy are presented in Section 3. The implications of this time dependent motion on the mixing and dispersion of passive tracers is discussed in Section 4. A discussion and summary of the results are given in Section 5.

2. Float tracks

The horizontal displacements of all floats which were not in Meddies are shown in Figure 2a superimposed on the climatological salinity at 1100 m from Levitus (1982). The float tracks demonstrate a variety of behavior, including low frequency zonal motions, oscillating wave-like motion, and looping indicative of mesoscale eddies. Two of the floats were carried to approximately 40W over a period of almost 4 years. As indicated in Figure 2a, this represents a significant portion of the zonal extent of the salt tongue. The summary of all float tracks indicates relatively strong eddy activity with non-homogeneous and non-isotropic distribution.

The net translation of the floats is indicated in Figure 2b. Most of the floats which were initially placed within the cluster at 32N, 24W were displaced to the west, or down the mean salinity gradient. While it is tempting to interpret this as an advective spreading of the salt tongue, we find that many others, some initially very close to the cluster floats, are displaced to the east, or up the mean salinity gradient. Furthermore, the current meter array K276 discussed by Müller and Siedler (1992) and Zenk and Müller (1988) indicates a westward mean flow at 33N, 22W over the lifetime of the floats (dashed line); however, the flow is to the east before and after the float experiment, giving a mean flow which is statistically not different from zero after 9 years. It is noted that some of the floats have undergone very little net translation over periods of years, indicative of very weak mean flows in this region. Figure 2b implies that mixing due to the time dependent motion must be important in maintaining the large-scale salt distribution.

Inspection of the individual trajectories reveals that floats that are near the core of the salt tongue show primarily a low frequency zonal motion, while floats to the south of the core show primarily a wave-like oscillatory motion that has a northwest to southeast polarization. This inhomogeneity is strong enough that in much of the subsequent analysis we compute statistics over subsets of "low frequency zonal

floats" and "wave-like floats." The data set is split about evenly between these two subsets. There is yet a third subset, Meddy floats, which includes 8 floats caught up in Meddies. These are excluded from the present analysis and mentioned only briefly (see Richardson *et al.,* 1989; and Armi *et al.,* 1989).

A summary of all the low frequency zonal floats is shown in Figure 2c. Of these 13 floats, 10 translated to the west and 3 to the east. The two floats which are carried far to the west appear to become trapped in mesoscale eddies (Richardson, 1993) while most of the other floats were advected rather smoothly over long distances. The northernmost float oscillates in an east-west pattern perpendicular to the mean salinity field several times before being advected up the gradient of the mean salt tongue. Similar zonal enhancement of the low frequency motion is predicted as the long time consequence of geostrophic turbulence on a beta-plane by Rhines (1975). A recent study by Spall (1993) suggests that baroclinic instability of the large-scale flow gives rise to low frequency zonal perturbations with spatial and temporal scales similar to what is observed here. In that study, the zonal orientation of the unstable waves results from the relatively weak vertical shear of the large-scale mean flow and the stabilizing influence of the planetary vorticity gradient for flows which are not zonal. The eddy density flux associated with this instability mechanism results in a rectified salt flux toward the west over the depth range of the salt tongue. A simple nonlinear model calculation indicates that this mechanism might be important in the overall salt balance in this region.

The tracks of the wave-like floats are summarized in Figure 2d. These patterns are quite different from the previous smooth zonal motions. They are almost all (10 out of 11) oriented in a northwest to southeast direction with positive Reynolds stresses ($\overline{u'v'} < 0$). It has been hypothesized by Spall (1992) that this is the signature of radiating Rossby waves generated to the south at the Cape Verde Frontal Zone (CVFZ). Such waves were characterized by periods of approximately 120 days, wavelengths of 315 km, and advective speeds of 1–5 cm s^{-1}. The presence of these oscillating patterns primarily in the south and east is consistent with their source being the CVFZ to the south. Waves of similar orientation were inferred from current meter data in this region by Siedler and Finke (1993). The present waves are relatively energetic with the eddy kinetic energy apparently much larger than the mean. Most (7 out of 10) of the wave floats were advected to the east, although for several this displacement is less than the apparent wavelength of the waves. An earlier or later sampling could have given a net westward translation.

The spatial coverage of the floats is insufficient to estimate a two dimensional picture of the mean horizontal flow field. Because the floats are distributed approximately along a meridional section, we averaged all of the float information within meridional bands to estimate the meridional pattern of the mean flow. The mean velocities were calculated by averaging the velocities of each of the floats which spent time within each latitude band, weighted by the appropriate number of days. The

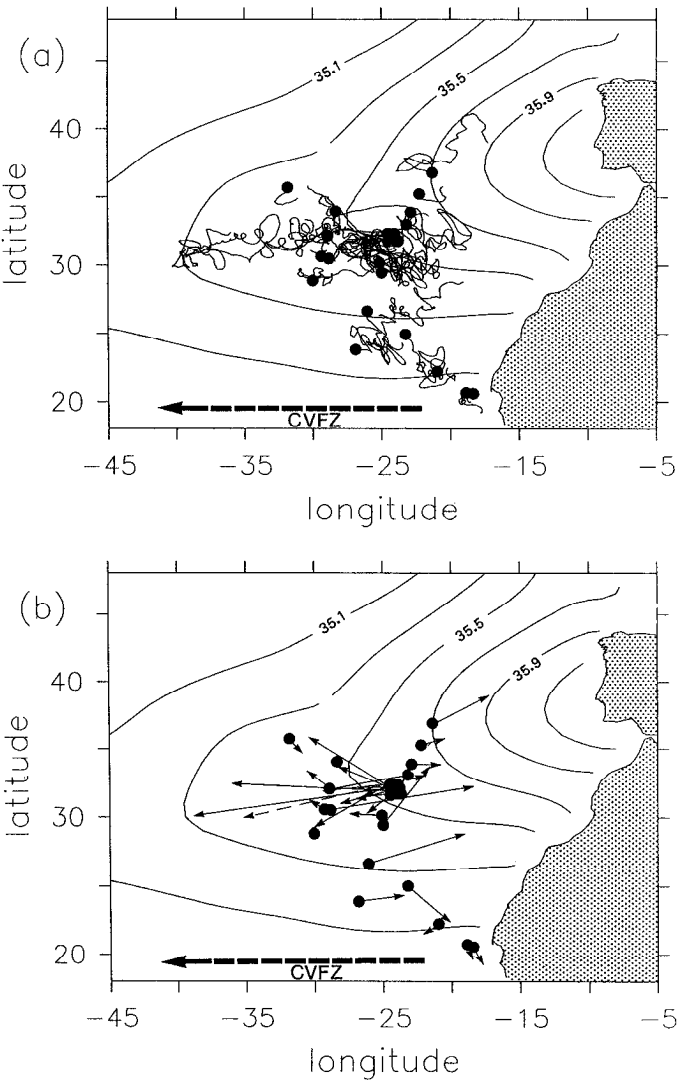

Figure 2. SOFAR float tracks superimposed on the climatological mean salinity field at 1100 m from Levitus (1982). The approximate location of the Cape Verde Frontal Zonal is also indicated. (a) all floats, (b) net displacements (dashed line indicates mean velocity at mooring K276 over duration of the SOFAR float experiment), (c) "zonal" floats, (d) "wave" floats.

advection of water masses due to Meddy displacements is not included in this mean; however, it does include the influences of any nearby Meddies on the surrounding flow.

The zonal average of the zonal and meridional velocities as a function of latitude is

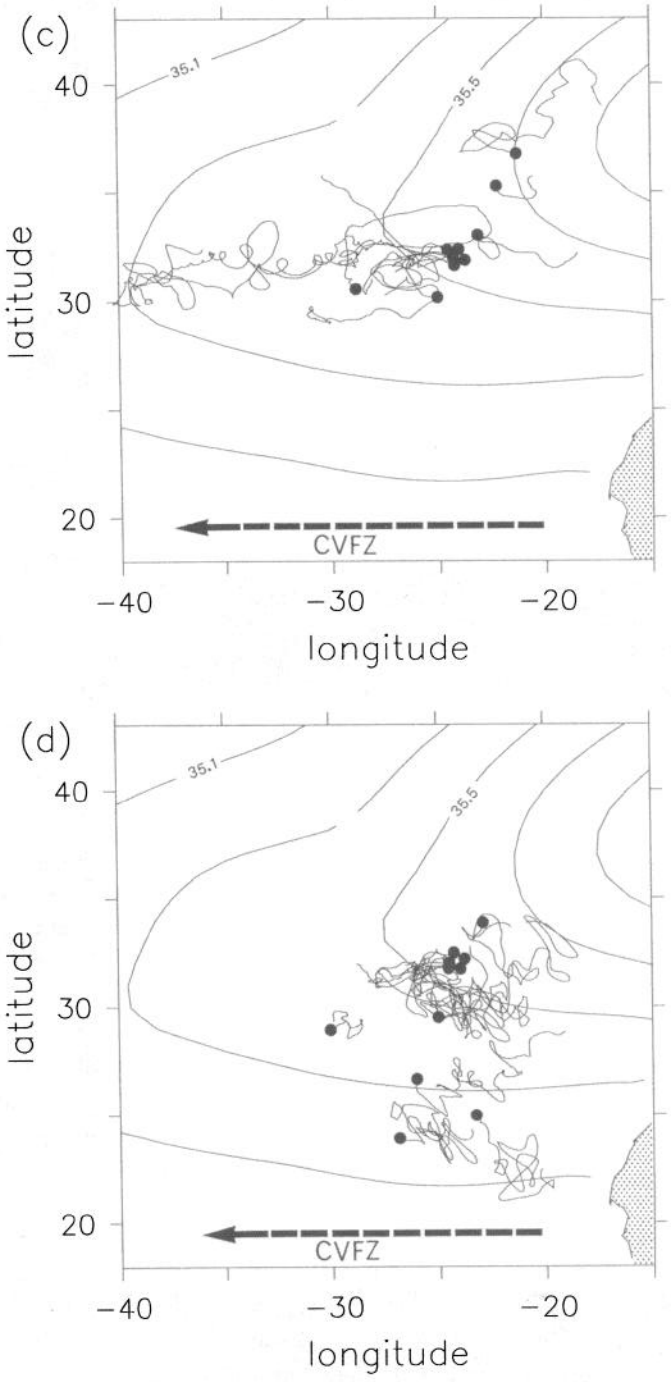

Figure 2. (Continued)

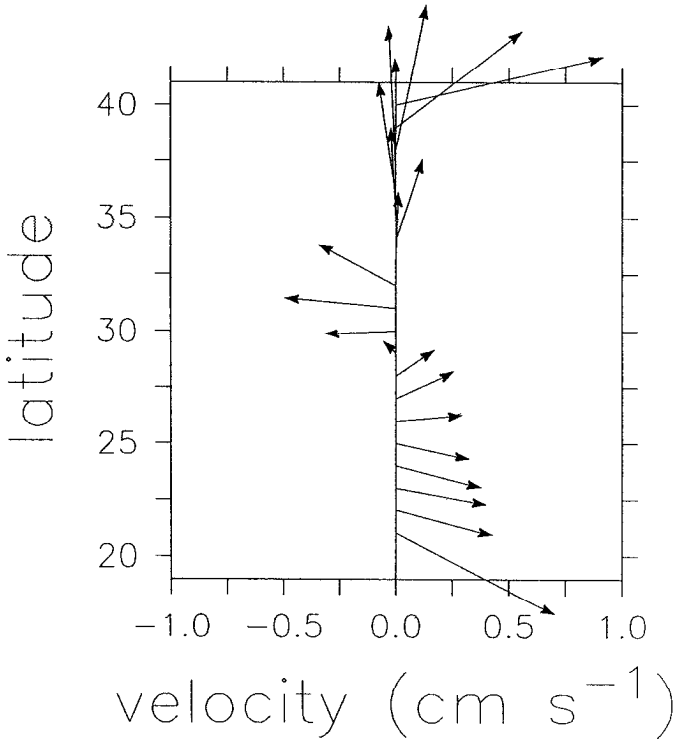

Figure 3. Mean velocity calculated from all SOFAR floats as a function of latitude.

shown in Figure 3. The distribution was smoothed three times by a three-point operator in order to give a large scale projection of the mean flow. A weak mean zonal flow of approximately 0.25 cm s^{-1} is found between 21N and 28N and the westward jet is evident between 30N and 32N with a strength of 0.5 cm s^{-1}. There is very little meridional flow south of 32N. North of this latitude the meridional flow is to the north of strength approximately 0.5 cm s^{-1}, in opposite direction to the upper ocean wind driven flow at this latitude. Such a northward flow at mid-depths in this region has also been found by Saunders (1982) and Maillard (1986). At the north the mean flow turns to the east. We note here that the mean north of approximately 35N is represented by only one float and, given that no floats were seeded to the north of this, it would be impossible to calculate a mean southward flow at these latitudes.

We note here that the uncertainties associated with these mean velocities are large and that they are not intended to represent a very long term mean flow for this region. We do believe, however, that they give a reasonable representation of the mean flow during the 3.5 years of the float experiment. The variability in this region is generally found to be much larger than the mean so that statistically significant mean flows are very difficult to obtain. In fact, in a nine year current meter record, Müller

and Siedler (1992) find that the mean zonal and meridional velocities at 1000 m are still not different from zero at the 95% confidence interval which they attribute to very low frequency fluctuations in the zonal component of the flow.

3. Eddy kinetic energy

a. Meridional distribution. The eddy kinetic energy (EKE) within each meridional band has been calculated by subtracting the velocity mean indicated in Figure 3 at the mean latitude of each float. The EKE as a function of latitude is shown in Figure 4a (solid line) together with various estimates based on current meter data (symbols). In general, the amplitudes of the EKE from the floats compare well with the current meter data, with values typically between 4 and 10 $cm^2\ s^{-2}$. The pattern of the meridional distribution also shows some similarities with maxima at 20–25N and 30–35N. These latitudes correspond to the upper ocean positions of the Cape Verde Frontal Zone in the south and the Azores Current in the north. A similar increase in EKE at mid-depths in the vicinity of these fronts was also reported by Müller and Siedler (1992). The regions on either side of these bands show a marked decrease in EKE in both the float data and the current meters, and are perhaps more representative of the natural variability of the subtropical gyre interior. The difference in EKE between the peaks and troughs are significant at the 95% confidence level. There is some indication of an increase at high latitudes, 38–40N, in the floats but this is based on very little float data so that the resulting uncertainties north of 35N are quite large, approximately 5 times larger than that for the middle latitudes indicated on the figure.

A similar meridional distribution of EKE is found in the Community Modelling Effort (CME) model. The CME model is an eddy resolving (⅓ degree latitude by ⅔ degree longitude resolution) basin scale primitive equation model forced by seasonal winds and surface buoyancy flux. The original calculation was carried out by Bryan and Holland (1989) at the National Center for Atmospheric Research as part of the World Ocean Circulation Experiment. The EKE at 1125 m calculated from the final 3 years of a 25 year integration is shown in Figure 4b. Although the amplitude of the EKE in the CME model is lower than in the float and current meter observations by a factor of approximately 5 (Spall, 1990), the meridional distribution is similar to that calculated from the float data. Two maxima are located at the latitudes of the CVFZ and the Azores Current with approximately equal strength minima between. The maximum related to the Azores Current is located slightly too far to the south in the model compared to the observations. This is consistent with the location of the Azores Current in the upper ocean of the model being south of the observed frontal position (Spall, 1990). The model clearly shows an increase in EKE to the north near 40N. This is believed to be a result of baroclinic instability of the upper ocean meridional flow (Spall, 1990; 1993). The realistic distribution of EKE found in the CME model result is significant to our interpretation of the float data. We can fairly

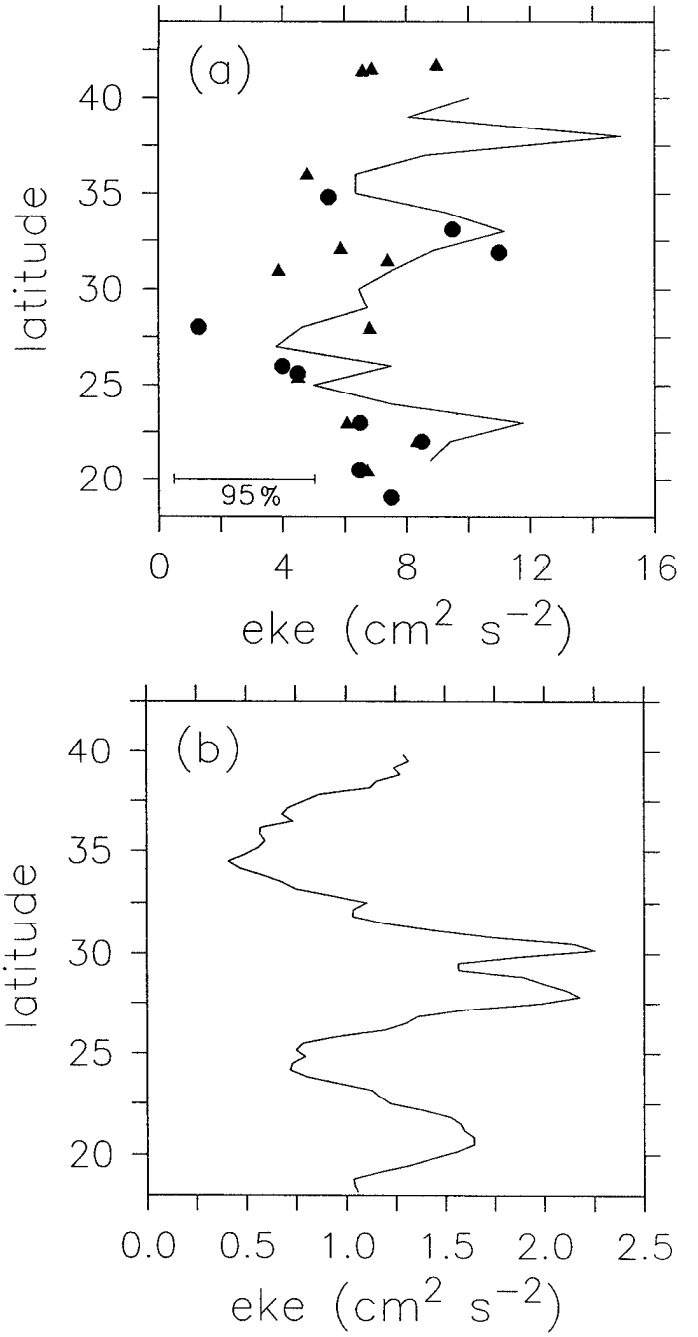

Figure 4. Eddy kinetic energy as a function of latitude. (a) solid line from SOFAR floats binned into 1 degree bands, the average 95% confidence interval between 22N and 36N is indicated. Symbols mark estimates from current meter data, ● from Müller and Siedler (1992), ▲ from Dickson (1989). (b) CME model at 1125 m, averaged between 20W and 40W.

easily describe the dynamics of the complete, three dimensional model fields, while we can see only the signatures of dynamical processes (e.g. spectral shapes) in the float data.

b. Spectral distribution. The eddy kinetic energy of each of the floats was calculated and binned into three frequency bands. The low frequency band contains all energy at periods longer than 200 days, the mesoscale band contains energy at periods between 50 days and 200 days, and the high frequency band contains all the energy at periods between 50 days and 2 days (the shortest period resolved by the data). The average spectral distribution of all those floats not in Meddies (21 total) is shown in Figure 5a. Only floats with lifetimes greater than 200 days were considered, although most were much longer than this (785 days on average) and 7 were longer than 3 years. The EKE is peaked in the mesoscale band with 6.3 $cm^2\ s^{-2}$ for the meridional component and 4.5 $cm^2\ s^{-2}$ for the zonal component. The low frequency band shows an enhancement of the zonal component (4.1 $cm^2\ s^{-2}$) over the meridional component (2.5 $cm^2\ s^{-2}$). The high frequency contribution is relatively weak and nearly isotropic. This amplitude and distribution is similar to that found in a two-year current meter record at the location of the cluster floats and is also typical of motions observed elsewhere in the interior of subtropical gyres (Schmitz *et al.,* 1988; Müller and Siedler, 1992).

Individual spectral distributions indicate that this mean distribution is not really representative of any of the floats, but rather an average of two very different types of behavior. The floats which exhibit a predominantly zonal motion (Fig. 2c) have a spectral distribution which is quite different from those which show wave-like behavior (Fig. 2d). The average spectral distribution of the low frequency zonal floats (Fig. 5b) indicates that the energy is still peaked in the mesoscale band but it is now nearly isotropic while the low frequency band is dominated by the zonal component (5.7 $cm^2\ s^{-2}$ versus 2.4 $cm^2\ s^{-2}$). The energy for the wave floats (Fig. 5c) is strongly peaked in the mesoscale band with the meridional component much larger than the zonal component (6.6 $cm^2\ s^{-2}$ versus 3.9 $cm^2\ s^{-2}$). The increased meridional component appears to be a result of the increased north-south orientation of the oscillations in most of the wave floats. The peak in the mesoscale band is consistent with the expected frequency of first mode baroclinic Rossby waves generated at the CVFZ (Spall, 1992). The low frequency band is nearly isotropic and close to the level of the meridional component for the zonal floats.

4. Horizontal mixing

From this relatively large data set we can attempt to estimate the horizontal mixing and mean advection by making use of the turbulent mixing ideas first introduced by Taylor (1921). The Lagrangian diffusivity may be expressed in terms of the time rate

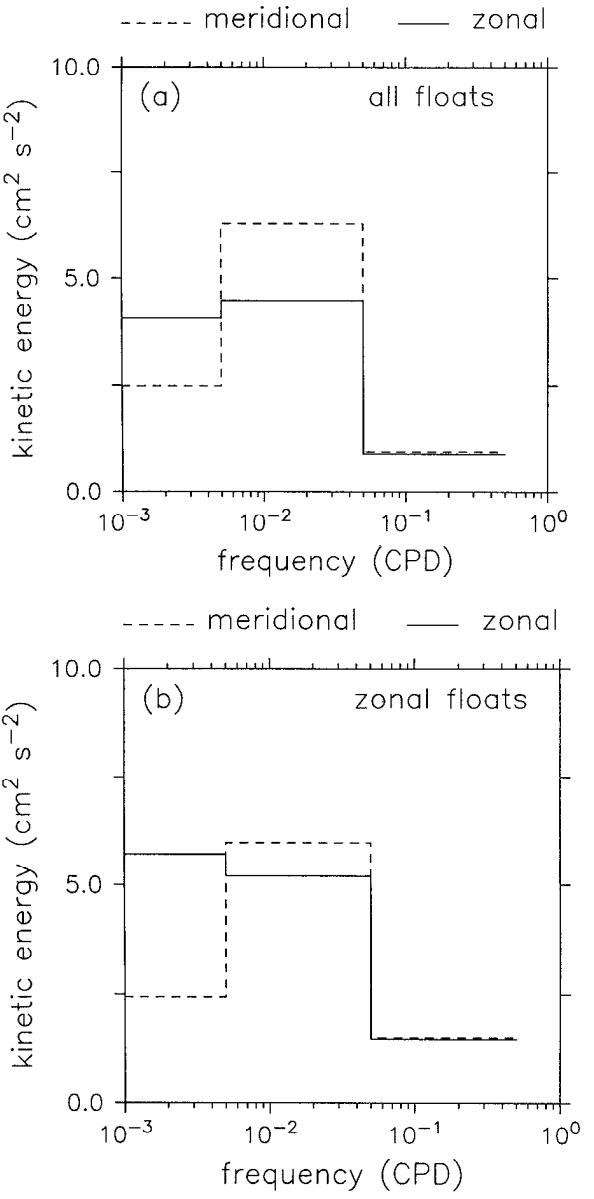

Figure 5. Spectral distribution of zonal and meridional kinetic energy binned into low frequency (greater than 200 day period), mesoscale frequency (50 to 200 days), and high frequency (less than 50 days). (a) all floats, (b) zonal floats, (c) wave floats.

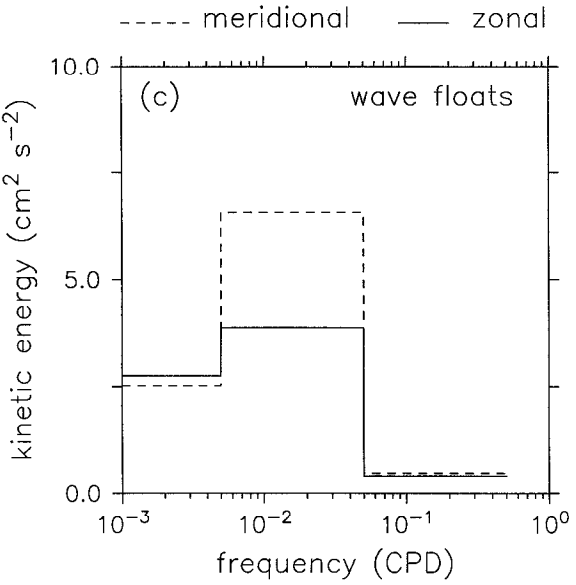

Figure 5. (Continued)

of change of the particle dispersion as

$$K_{ii} = \frac{1}{2}\frac{d\overline{x_i'^2}}{dt}, \tag{1}$$

where the overbar denotes the time average, the prime corresponds to departures from the mean, and the subscript $i = 1, 2$ corresponds to the zonal and meridional directions. Taylor showed that for long times in a homogeneous, stationary turbulent field, (1) may be approximated by

$$K_{ii}^{*} = \langle\overline{u_i'^2}\rangle T_i, \tag{2}$$

where $\langle\overline{u_i'^2}\rangle$ is the velocity variance and T_i is the integral time scale. The angle brackets indicate an ensemble average over all Lagrangian parcels. The Lagrangian integral time scale may be calculated from the Lagrangian autocorrelation function R_i as

$$T_i = \int_0^{\infty} R_i(\tau)\, d\tau, \tag{3}$$

where

$$R_i(\tau) = \frac{\langle u_i'(\tau)u_i'(t+\tau)\rangle}{\langle u_i'^2\rangle} \tag{4}$$

is a measure of the time for which fluid parcels remember their previous state. The

primes indicate than a mean velocity has been subtracted from the Lagrangian velocities. For very short times $R_i \rightarrow 1$ while for very long time $R_i \rightarrow 0$. Thus, if the time scales of the flow are well resolved by the Lagrangian float trajectories, the integral of R_i will approach a constant value and the integral time scale is well defined.

The separation between mean and eddy velocities implied by u' is important, and, in the end, comes down to a judgment. With very sparsely spaced floats, and lacking additional data, one might assume that the mean velocity of each float is representative of the regional mean and simply subtract this from each float to obtain the time dependent component of the flow. This approach makes less sense, however, if one is measuring the long time dispersion of a group of floats because the mean velocity of each float may be quite different even though their mean locations are similar. This would imply that the mean velocity field has significant variability on small scales, which is unlikely away from stationary frontal regions. In order to address this problem, we have chosen to define a mean velocity as a function of position taking into account all of the float data, hence, the residual velocities have been determined by subtracting the mean velocities in Figure 3 at the mean latitude of each of the floats.

One of the underlying assumptions of Taylor's relationship (2) is that the turbulent velocity field is homogeneous. Because the float trajectories indicate that the wave motions are dominant to the south and east, and the low frequency zonal motions are found to the north and west, it is apparent that the eddy field in this region is not homogeneous. However, because there also appears to be a fairly clear geographical and phenomenological distinction between trajectory types, we will treat the low frequency zonal floats and the wave-like floats separately.

a. Integral time scales. The zonal and meridional autocorrelation functions for the wavelike floats are shown in Figure 6a. These representative curves were calculated by averaging the individual autocorrelation functions for each of the wave floats with lifetimes greater than 516 days (9 total). The functions show negative lobes for both components, as expected for wave-like variability. The maximum negative correlations at 50–60 days is consistent with the expected period of 120 days for the first mode baroclinic Rossby waves predicted by Spall (1992). The zero crossings for the zonal and meridional components are 41 and 30 days, respectively.

The average zonal and meridional autocorrelation functions for the low frequency zonal floats is shown in Figure 6b. For these floats (8 total with lifetimes greater than 381 days), we find a much different pattern. The zero crossings are at later times (110 and 47 days for zonal and meridional components) and there are no strong negative lobes as found for the wave floats. This positive correlation for over 100 days for the zonal flow is quite long for oceanic variability, even at 1000 m depth. For times greater than 125 days the velocities are essentially uncorrelated.

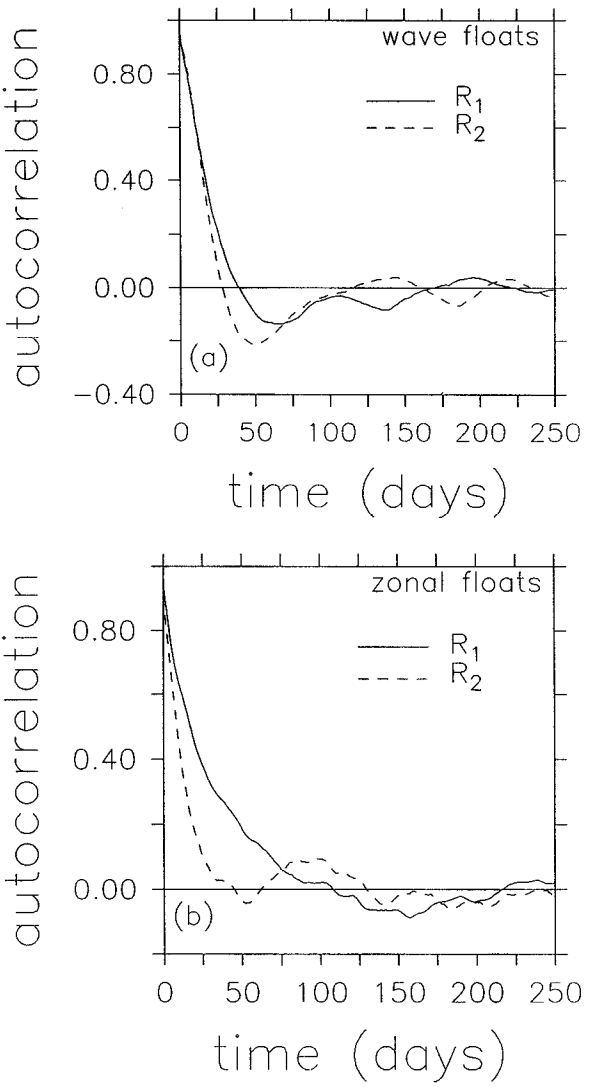

Figure 6. Autocorrelation function for (a) wave floats and (b) zonal floats. Solid lines indicate zonal component, dashed lines indicate meridional component.

The Lagrangian integral time scales calculated from the autocorrelation functions using Eq. 3 are shown in Figure 7a and b as a function of integration time. The time scale for the waves increases rapidly to about 15 days for both components. Due to the wavelike nature of the variability, however, the integral time scales are decreased as the wave goes through a full period. After approximately 150 days the autocorrelations are very small and the integral time scales are essentially constant, (ie. the integrals converge). The integral time scales averaged between 150 and 250 days are

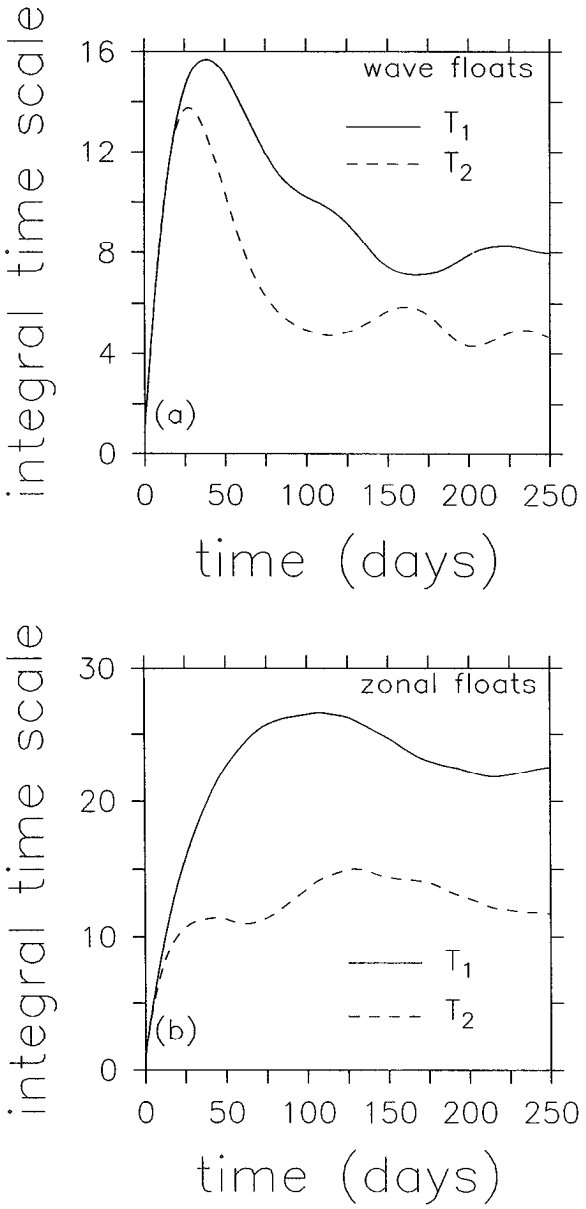

Figure 7. Integral time scale (days) versus integration time for (a) wave floats and (b) zonal floats. Solid lines indicate zonal component, dashed lines indicate meridional component.

7.7 and 5.0 days for the zonal and meridional components, respectively. The integral time scales for the zonal floats (Fig. 7b) increase almost asymptotically to much larger values than the wave floats. The average time scales between 150 and 250 days are 23 and 13 days. We note that the Lagrangian integral time scales did not converge

Table 1. Lagrangian statistics and eddy diffusivities for the zonal floats and wave floats. 95% confidence limits are indicated in brackets. The horizontal diffusivity K_{ii}^* is based on Taylor's relation (2) while K_{ii} is a direct estimate from the float dispersion (Eq. (1)), $i = 1, 2$ indicates zonal and meridional directions.

GROUP	i	$\langle u_i'^2 \rangle$ (cm^{2}s^{-2})	T_i (days)	K_{ii}^* (10^6 cm^{2}s^{-1})	K_{ii} (10^6 cm^{2}s^{-1})
WAVE	1	6.2 (5.8,6.7)	7.7	4.3 (3.9,4.6)	5.7 (4.3,6.7)
WAVE	2	7.6 (7.2,8.1)	5.0	3.5 (3.3,3.8)	4.0 (3.8,4.4)
ZONAL	1	10.6 (8.9,12.7)	23	21 (18,25)	26 (20,30)
ZONAL	2	8.1 (7.2,9.2)	13	8.4 (7.4,9.6)	8.0 (7.9,11)

to uniform values when the residual float velocities were calculated based on the mean velocity of each float instead of the spatial mean used here.

These integral time scales span what has typically been calculated for mid-depth oceanic mesoscale variability. Freeland *et al.* (1975) calculated time scales of 12 and 10 days at 1500 m in the MODE area (near 28N, 70W). Böning and Cox (1988) calculated time scales of approximately 13 and 9 days using simulated Lagrangian trajectories within the subtropical gyre of a basin scale primitive equation model. The present wavelike motions have much smaller time scales, while the zonal component of the zonal floats has a time scale much larger than that reported previously. Time scales near the surface have been found to have shorter time scales on the order of 2–4 days, at least partially as a result of the surface intensification of kinetic energy (Krauss and Böning, 1987).

b. Lagrangian diffusivities. Estimates of the horizontal diffusivity calculated from Eq. 2 are shown in Table 1 for K_{ii}^*. The velocity variances were obtained from the residual velocity fields used to calculate the autocorrelation functions. The number of degrees of freedom used to estimate the confidence intervals was taken as the number of integral time periods (T_i) contained in the total time represented by the sum of all the floats in each group. Although there are statistically significant differences between the EKE levels, they are all of similar magnitude with the zonal floats slightly more energetic than the wave floats. However, the considerable difference in integral time scales results in much different effective eddy diffusivities. The diffusivities of the wave floats are small, as expected for motions which are periodic in nature, while the zonal floats are more effective at mixing. The mixing coefficient in the zonal direction is about five times larger than for the wave floats. The meridional component is somewhat lower, but still a factor of two larger than for the waves. The confidence limits for the diffusivities were calculated based on the confidence limits of the velocity variance only, assuming the integral time scale is well known. The actual confidence intervals would be somewhat larger if uncertainties in the time scales were also taken into account. Nonetheless, the differences between mixing coefficients for each float group are large enough to be significant even

considering reasonable errors in the time scales. These estimates are slightly larger than the $1 - 5 \times 10^6$ cm^2 s^{-1} obtained by Hogg (1987) using an inverse model in this region. The zonal value is close to the range of $15 - 30 \times 10^6$ cm^2 s^{-1} estimated by Needler and Heath (1975). Lagrangian observations at mid-depths in the western North Atlantic indicate that the diffusivities are between 7 and 15×10^6 cm^2 s^{-1} and nearly isotropic (Freeland *et al.,* 1975; Rossby *et al.,* 1983). Böning and Cox obtain estimates of $(K_{xx}, K_{yy}) = (20, 1) \times 10^6$ cm^2 s^{-1} at 1000 m in the eastern basin of a North Atlantic numerical model. The present diffusivities are somewhat smaller and less isotropic than those calculated in the western North Atlantic, but similar to those modelled in the eastern basin.

We tested the validity of Taylor's approximation to the long time limit (Eq. 2) by calculating the diffusion coefficients directly from the particle dispersions (Eq. 1). Each of the float trajectories was broken up into 250-day segments, with each segment treated as an independent sample. An estimate of the long time diffusivity was obtained by calculating the average time rate of change of the dispersion over each of the 250-day periods. Confidence limits were calculated using the total number of 250-day segments in each float group. The average diffusivities for each float group and direction are given in Table 1 for K_{ii}. The direct estimates are nearly the same as the indirect estimates based on Taylor's relation (within the 95% confidence limits). This indicates that the floats are essentially in a random walk regime for long times and gives confidence to our assumption that the mixing is well represented by stationary homogeneous turbulence, at least for time scales of 250 days.

c. Particle dispersion—Mean and eddy contributions. The amplitudes of the horizontal diffusion coefficients are only a partial indication of the importance of eddy mixing in the transport of water parcels. Here we compare the ratio of the displacement due to mean advection to the root mean square displacement due to random mixing by the turbulent eddy field, written as

$$b_i(t) = \frac{\langle |\overline{U_i}| \rangle t^{1/2}}{(2 \langle \overline{u'^2} \rangle T_i)^{1/2}} \tag{5}$$

The mean velocity $\overline{U_i}$ was taken from the average latitude of each float, the velocity variance $\overline{u'^2}$ estimated from the residual velocities for each float, and the integral time scale T_i from Table 1. The ratio b is plotted in Figure 8 as a function of time. The relative importance of the mean component increases with the square root of time so that eventually the mean flow will always dominate the particle dispersion. After 5 years, however, the eddy component is still dominant over the mean component for all spreading except in the zonal direction for the wave floats. Even in this case, however, the eddy component is still responsible for over 50% of the dispersion.

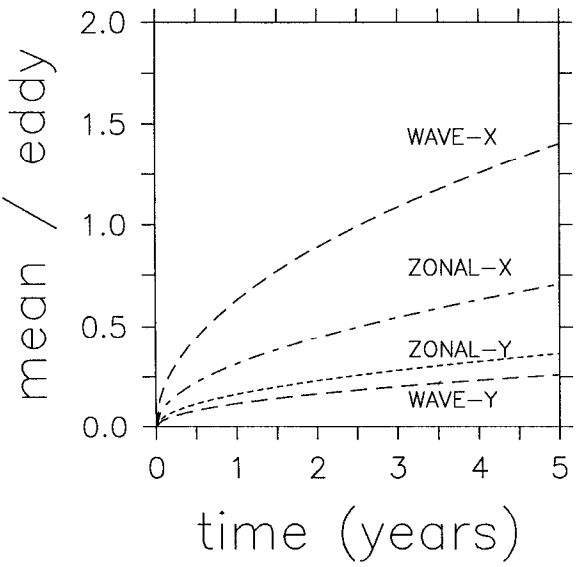

Figure 8. Ratio of mean to eddy contributions for particle dispersion, from Eq. (5).

These results indicate that, over the time scale of the experiment, the dispersion of the floats is dominated by turbulent mixing, in contrast to the numerical study of Böning and Cox (1988) where they found that the mean flow was dominant after less than ½ year. This may be due to too little eddy kinetic energy in the model compared to the observations. The ratio for the meridional components of both the zonal and wave floats is very small, indicating that eddy mixing plays an important role in the meridional spreading of properties at mid-depths in the eastern basin at these latitudes. The usefulness of this ratio for time scales longer than several years is questionable because the mean flow used in the calculation is probably not representative of the long term (decadal) mean. We anticipate that additional data would result in smaller mean velocities, particularly in the core of the salt tongue, and an even larger contribution due to the time dependent motion.

5. Discussion and conclusions

Long time series of quasi-Lagrangian float trajectories have revealed two distinct types of low frequency variability at mid-depths in the Canary Basin of the North Atlantic. There appears to exist a fairly clear geographical separation, with the variability within the core of the Mediterranean salt tongue dominated by very low frequency zonal motions and mesoscale eddies, and the variability to the south of the tongue core dominated by wave-like oscillations with periods on the order of 120 days. It has been hypothesized that the wave-like oscillations are the signature of baroclinic Rossby waves originating at the Cape Verde Frontal Zone to the south

(Spall, 1992) and that the zonal motions are the signature of baroclinic instability of the large-scale flow (Spall, 1993).

The influences of this time dependent motion on the mixing and dispersion of tracers has been investigated. We have made use of the theory of mixing due to homogeneous, stationary turbulence (Taylor, 1921) to estimate the effective diffusivity for the zonal and the wave-like motions. It is shown that the low frequency zonal motions are much more effective at mixing than are the waves even though their energy levels are similar. The zonal velocity of the advective floats is, on average, positively correlated for 110 days, much longer than is typically found for mesoscale variability, even at mid-depths in the ocean. This results in long integral time scales (23 and 13 days) and large diffusivities (21 and 8.4×10^6 cm^2 s^{-1}) for the zonal and meridional components. The wave motions have a strong negative correlation at times between 50 and 120 days, as expected for oscillations with a period of 120 days, which result in short integral time scales (7.7 and 5.0 days) and low diffusivities ($3 - 4 \times 10^6$ cm^2 s^{-1}). This is a consequence of the wave dynamics and stresses the importance of integrating the autocorrelation function beyond the first zero crossing. Although an isolated, linear wave packet would result in no mixing, the present waves are only approximately linear and they interact with the surrounding water on a wide range of space and time scales. Because of the large differences in integral time scales, the mixing coefficients do not simply scale with the eddy kinetic energy, as has been found elsewhere in the ocean (Rossby *et al.,* 1983; Krauss and Böning, 1987).

These results imply that mixing due to the time dependent motion is both non-homogeneous and non-isotropic. The non-homogeneity results from the zonal motions being found within the core of the salt tongue, and the wave motions existing mostly to the south and east. This distribution is consistent with the source of the waves being the Cape Verde Frontal Zone at approximately 20N. The group velocity of Rossby waves propagates their energy toward the north and east, into the region where the floats were seeded and into the southern extent of the salt tongue. As a result of this energy propagation, we find some overlap in the regions where the two types of motion exist. We expect to find the strongest low frequency zonal motions driven by baroclinic instability in regions where the upper ocean flow is north-south, as it is at the latitudes of the salt tongue. The lack of zonal motions to the south is consistent because the large scale, upper ocean flow is stabilized as it turns to the west south of the salt tongue. The phase speeds of zonal perturbations which result from baroclinic instability are nearly zero so that they would not propagate significantly away from their source region. The non-isotropic nature of the diffusivity is enhanced in the region where baroclinic instability of the large-scale flow is the dominant source of variability because of the stabilizing influence of the planetary vorticity gradient.

The data coverage here is not sufficient to make reliable estimates of the salt

balances within the salt tongue mainly because the zonal mean flow is small and its estimation requires very long time averaging. It is nevertheless clear that eddy mixing plays a crucial role. Zonally enhanced eddy mixing may account for the zonal elongation of the salt tongue, although mean flows which are smaller than we can reliably measure could also account for this asymmetry. The meridional gradient of eddy diffusivity between the region of zonal motion and the region of wave motion may be thought of as a mean flow of approximately 1 mm s^{-1} from the core of the salt tongue toward the south. This is the same order of magnitude as the estimated mean flows in the region and indicates that spatial variations in diffusivity may be important.

While we have provided a glimpse of the complex variability within the salt tongue, it is clear that additional observations and more comprehensive models are needed if we are to reliably estimate the salt balances within the Mediterranean salt tongue. The present analysis has implicitly assumed that salinity may be thought of as a passive tracer, although this is not really true as saline effects are not neglegible in the equation of state. Meddies are lenses of very salty water which are not passivly advected with the surrounding flow but are influenced by their own vortex dynamics and interaction with the upper ocean flow. A simple order of magnitude analysis indicates that they are not neglegible in the overall salt balance. If the zonal motions observed here are the signature of baroclinic instability, then they may also have a rectified westward flux of salt at the depths of the salt tongue which is not neglegible (Spall, 1993). We have concentrated on horizontal processes in the present study, although vertical fluxes of salt are also likely to be important in the overall balance.

Acknowledgments. This work was supported by NSF Grant No. OCE-9009463. Chris Wooding calculated the spectral distributions of EKE from the float data. Frank Bryan and Bill Holland are thanked for supplying the CME model output which was used to calculate Figure 4b. Final revisions to the manuscript were made while MAS was at the Institut für Meereskunde in Kiel, Germany. This is contribution number 8329 from the Woods Hole Oceanographic Institution.

REFERENCES

Armi, L. and D. Haidvogel. 1982. Effects of variable and anisotropic diffusivities in a steady state diffusion model. J. Phys. Oceanogr., *12,* 785–794.

Armi, L., D. Herbert, N. Oakey, J. F. Price, P. L. Richardson, H. T. Rossby and B. Ruddick. 1989. Two years in the life of a Mediterranean Salt Lense. J. Phys. Oceanogr., *19,* 354–370.

Böning, C. W. and M. D. Cox. 1988. Particle dispersion and mixing of conservative properties in an eddy resolving model. J. Phys. Oceanogr., *18,* 320–338.

Bryan, F. O. and W. R. Holland. 1989. A high resolution simulation of the wind- and thermohaline-driven circulation of the North Atlantic Ocean. Proceed. Hawaiian Winter Workshop: Parameterizations of small scale processes. Univ. of Hawaii, Jan 17–20.

Defant, A. 1955. Die Ausbreitung des Mittelmeerwassers im Nordatlantischen Ozean. Deep-Sea Res., 465–470.

Dickson, R. 1989. Flow statistics from long-term current meter moorings: The Global data-set in January 1989. MAFF Directorate of Fisheries Research, Lowestoft, England. World Meteorological Organization Technical Document No. 337, 414 pp.

Freeland, H. J., P. Rhines and H. T. Rossby. 1975. Statistical observations of trajectories of neutrally buoyant floats in the North Atlantic. J. Mar. Res., *33,* 383–404.

Haidvogel, D. B. and T. Keffer. 1984. Tracer dispersal by mid-ocean eddies. Part I: Ensamble statistics. Dyn. Atmos. Oceans, *8,* 1–40.

Hogg, N. G. 1987. A least-squares fit of the advective-diffusive equations to Levitus Atlas data. J. Mar. Res., *45,* 347–375.

Krauss, W. and C. W. Böning. 1987. Lagrangian properties of eddy fields in the North Atlantic as deduced from satellite-tracked buoys. J. Mar. Res., *45,* 259–291.

Levitus, S. 1982. Climatological atlas of the world ocean. NOAA Prof. Paper, *13,* 173 pp.

Maillard, C. 1986. Atlas hydrologique de l'Atlantic Nort-Est. Institut Francais de Recherche pour l'Exploitation de la Mer. Brest, 32 pp.

Müller, T. J. and G. Siedler. 1992. Multi-year current time series in the eastern North Atlantic ocean. J. Mar. Res., *50,* 63–98.

Needler, G. T. and R. A. Heath. 1975. Diffusion coefficients calculated from the Mediterranean salinity anomaly in the North Atlantic. J. Phys. Oceanogr., *5,* 173–182.

Rhines, P. B. 1975. Waves and turbulence on a beta-plane. J. Fluid Mech., *69,* 417–443.

Richardson, P. L. 1993. A census of eddies observed in North Atlantic SOFAR float data. Prog. Oceanogr., *31,* 1–50.

Richardson, P. L. and K. Mooney. 1975. The Mediterranean outflow—a simple advection—diffusion model. J. Phys. Oceanogr., *5,* 476–482.

Richardson, P. L., D. Walsh, L. Armi, M. Schröder and J. F. Price. 1989. Tracking three Meddies with SOFAR floats. J. Phys. Oceanogr., *19,* 371–383.

Riser, S. C. and H. T. Rossby. 1983. Quasi-Lagrangian structure and variability of the subtropical western North Atlantic circulation. J. Mar. Res., *41,* 127–162.

Rossby, H. T., S. C. Riser and A. J. Mariano. 1983. The western North Atlantic—A Lagrangian view, *in* Eddies in Marine Science, A. R. Robinson, ed., Springer-Verlag, New York, 609 pp.

Saunders, P. M. 1982. Circulation in the eastern North Atlantic. J. Mar. Res., *40,* 641–657.

Schmitz, W. J., J. F. Price and P. L. Richardson. 1988. Recent moored current meter and SOFAR float observations in the eastern Atlantic near 32N. J. Mar. Res., *46,* 301–319.

Siedler, G. and M. Finke. 1993. Long period transport changes in the eastern North Atlantic and their simulation by propagating waves. J. Geophys. Res., *98(C2),* 2393–2406.

Spall, M. A. 1990. Circulation in the Canary basin: A model/data analysis. J. Geophys. Res., *95,* 9611–9628.

—— 1992. Rossby wave radiation in the Cape Verde Frontal Zone. J. Phys. Oceanogr., *22,* 796–807.

—— 1993. A mechanism for low frequency variability and salt flux in the Mediterranean salt tongue. J. Geophys. Res., (submitted).

Taylor, G. I. 1921. Diffusion by continuous movement. Proc. Lond. Math. Soc., *20,* 196–212.

Zemanovic, M. E., P. L. Richardson and J. F. Price. 1990. SOFAR float Mediterranean outflow experiment summary and data from 1986–1988. Woods Hole Oceanographic Technical Report, WHOI-90-01, 239 pp.

Zenk, W. and T. J. Müller. 1988. Seven year current meter record in the eastern North Atlantic. Deep-Sea Res., *35,* 1259–1268.

Received: *18 February, 1993;* revised: *17 August, 1993.*